

A Nonlinear State-Space Model of a Combined Cardiovascular System and a Rotary Pump

Antonio Ferreira, *Student Member*, Shaohui Chen,

Marwan A. Simaan, *IEEE Fellow*, J. Robert Boston, *IEEE Member*, James F. Antaki, *IEEE Member*

Abstract—A nonlinear lumped parameter model of the cardiovascular system coupled with a rotary blood pump is presented. The blood pump is a mechanical assist device typically interposed from the left ventricle to the aorta in patients with heart failure. The cardiovascular part of the model (consisting of the left heart atrium and ventricle), and the systemic circulatory system are implemented as an RLC circuit with two diodes. The diodes represent the mitral and aortic valves in the left heart. The cardiovascular model has been validated with clinical data from a patient suffering from cardiomyopathy. The pump model is a first order differential equation relating pressure difference across the pump to flow rate and pump speed. The combined cardiovascular-pump model has been represented as a fifth order nonlinear dynamical system in state space form with pump speed as the control variable. This model was used to simulate the hemodynamic variables to different values of afterload and a linearly increasing (ramp) pump speed. Because of its small dimensionality, the model is suitable for both parameter identification and the application of modern control theory.

I. INTRODUCTION

The human cardiovascular system is a time-varying distributed parameter nonlinear system. Nevertheless, lumped-parameter mathematical models of the cardiovascular system have been developed for many years for a variety of purposes. These include estimation and study of cardiovascular parameters difficult to measure in practical situations and analysis and development of new medical products.

Zacek et al [1] modeled the human cardiovascular system as 15 elements (tubes) connected in series representing the main parts of the system, with rigid and elastic reservoir components. This model provided reasonable results, even at higher and varying heart rates. Voytik et al [2] developed an electrical model of the human circulatory system to investigate a variety of designs for an accessory skeletal muscle ventricle (SVM). Three different configurations of the SVM were simulated as counterpulsatile assist devices for both normal and congestive heart failure. Avanzolini et al [3] use computer aided design of control system (CADCS) to simulate the human cardiovascular system steady-state response. Transients were introduced by varying the peripheral resistance.

This research was supported in part by NSF under contract ECS-0300097 and NIH/NHLBI under contract 1R43HL66656-01

A. Ferreira and S. Chen are graduate students at the Department of Electrical Engineering, University of Pittsburgh, PA, USA.

M. A. Simaan and J. R. Boston are with the Department of Electrical Engineering, University of Pittsburgh, PA, 15261 USA.

J. F. Antaki is with the Department of Biomedical Engineering, Carnegie Mellon University, Pittsburgh, PA 15213 USA.

Recently, mathematical models of the human circulation have been developed also for studying its interaction with assist devices. Bai et al [4] presented a cardiovascular system model which includes a simulation of a cardiac assist device by external counterpulsation. It includes the left and right heart and the pulmonary circulation. De Lazzari et al [5] studied the interaction between a pneumatic left ventricle assist device (LVAD) and the cardiovascular system, by using energy variables, such as external work, oxygen consumption and cardiac mechanical efficiency for both fixed and variable heart rates. Computer models [6], [7] have been useful for simulating the interaction between the human cardiovascular system and assist devices, prior to in vitro and in vivo experiments. However, control strategies derived from such complex models have not been implemented due to the many state variables that are not observable in practice. For the same reason, on-line identification of cardiovascular parameters remains a difficult task.

To apply modern control techniques the cardiovascular-pump model must be formulated in terms of state-space description. Thus, our main purpose in this paper is to describe the nonlinear cardiovascular-pump model in a state-space form, suitable for the direct application of modern control techniques.

The paper is organized as follows: Section II describes the heart model, its parameters and the left ventricular pressure-volume relationship. Section III presents the cardiovascular-pump model and its state space description. Section IV shows how the heart model was validated and shows the hemodynamic tests performed with both models. Finally, results are discussed and further improvements are suggested.

II. CARDIOVASCULAR MODEL

One advantage in representing the cardiovascular model as a lumped circuit is that Kirchoff's laws for node currents and loop voltages can be applied. In doing so, we can relate current with flow and voltage with pressure. Moreover, components like resistors, capacitors and inductors can be associated with hydraulic resistance, compliance and inductance, respectively. The cardiovascular model can therefore be represented as a lumped parameter electric circuit [8],[9] as shown in Figure 1. Preload and pulmonary circulation are represented by a single compliance and afterload by a four-element Windkessel model. Table I lists the state variables employed, and Table II provides the system parameters and their associated values.

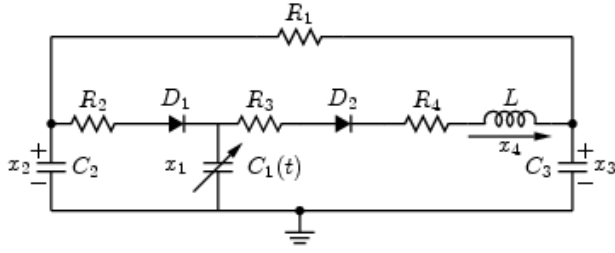


Fig. 1. Cardiovascular Model

TABLE I
STATE VARIABLES

Variables	Name	Physiological Meaning (unit)
x_1	LVP	Left Ventricular Pressure (mmHg)
x_2	LAP	Left Atrial Pressure (mmHg)
x_3	AP	Arterial Pressure (mmHg)
x_4	Q_A	Aortic flow (ml/sec)

TABLE II
MODEL PARAMETERS

Parameter	Value	Physiological Meaning
Resistances (mmHg.sec/ml)		
R_1	variable	Systemic Vascular Resistance (SVR). Its value depends on the level of activity of the patient
R_2	0.005	Mitral valve resistance
R_3	0.001	Aortic valve resistance
R_4	0.0398	Characteristic resistance
R_5	0.0677	Cannulae inlet resistance
R_0	0.0677	Cannulae outlet resistance
Compliances (ml/mmHg)		
$C_1(t)$	time-varying	Left ventricular compliance $C_1(t) = 1/E(t)$, equation (1)
C_2	4.4	Left Atrial compliance
C_3	1.33	Systemic compliance
Inertance (mmHg.sec ² /ml)		
L	0.0005	Inertance of blood in Aorta
L_1	0.0127	Cannulae inlet inertance
L_0	0.0127	Cannulae outlet inertance
Valves		
D_1		Mitral valve
D_2		Aortic valve

A. The Left Ventricle

In our lumped parameter circuit, the left ventricle is described as a time-varying capacitor. One way to model its behavior is by means of the elastance function, which is the reciprocal of the compliance. It determines the change in pressure for a given change in volume within a chamber and was defined following Suga and Sagawa as [10]

$$E(t) = \frac{LVP(t)}{LVV(t) - V_0} \quad (1)$$

where $E(t)$ is the time varying elastance (mmHg/ml), $LVP(t) = x_1(t)$ is the left ventricular pressure (mmHg), $LVV(t)$ is the left ventricular volume (ml) and V_0 is a reference volume (ml), the theoretical volume in the ventricle at zero pressure.

Several mathematical approximations have been used to implement the elastance function. In this work, we use:

$$E(t) = (E_{max} - E_{min}) \cdot E_n(t_n) + E_{min} \quad (2)$$

where $E_n(t_n)$ is the so called ‘‘double hill’’ function [11] function:

$$E_n(t_n) = 1.55 \left[\frac{\left(\frac{t_n}{0.7}\right)^{1.9}}{1 + \left(\frac{t_n}{0.7}\right)^{1.9}} \right] \left[\frac{1}{1 + \left(\frac{t_n}{1.17}\right)^{21.9}} \right] \quad (3)$$

In the above expression, $E_n(t_n)$ is the normalized time-varying elastance, $t_n = \frac{t}{T_{max}}$, $T_{max} = 0.2 + 0.15tc$ and tc is the cardiac cycle interval, i.e. $tc = 60/HR$, where HR is the heart-rate. Notice that $E(t)$ is a re-scaled version of $E_n(t_n)$ and the constants E_{max} and E_{min} are related to the end-systolic pressure volume relationship (ESPVR) and the end-diastolic pressure volume relationship (EDPVR), respectively. Figure 2 shows $E(t)$ for $E_{max} = 2.0$, $E_{min} = 0.06$, and heart-rate 75 beats per minute (bpm).

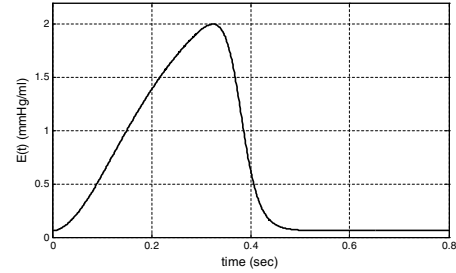


Fig. 2. Elastance function for a heart rate of 75 bpm

Another suitable definition for the states of the system is

$$z = [z_1, \dots, z_4]^T = [LVV(t) - V_0, LAP, AP, Q_A]^T \quad (4)$$

which has left ventricular volume as the first state variable instead of left ventricular pressure. As we will show later, there may be a computational advantage in using the z state variables instead of the x state variables.

Note that the x and z vectors are related by the transformation $x = Pz$, where the matrix P is defined as

$$P(t) = \begin{bmatrix} E(t) & \vdots & \mathbf{0} \\ \dots & \dots & \dots \\ \mathbf{0} & \vdots & I_3 \end{bmatrix} \quad (5)$$

where I_3 is the third order identity matrix. Using standard circuit methodology (KVL, KCL, etc) the state equations for the model in Figure 1 can be written in the form of $\dot{x} = A_1(t)x$. The same equation can also be transformed to the z state vector, and will be written as $\dot{z} = A_2(t)z$. It can be easily shown that the $A_1(t)$ and $A_2(t)$ matrices are related by

$$A_2(t) = P^{-1}(t)A_1(t)P(t) - P^{-1}(t)\dot{P}(t) \quad (6)$$

Since our circuit model of Figure 1 includes two diodes (switches representing the valves in the left side of the heart) the following 3 phases will occur, over four different time intervals, as illustrated in Table III.

TABLE III
PHASES OF THE CARDIAC CYCLE

Modes	Valves		Phases
	D_1	D_2	
1	closed	closed	Isovolumic contraction
2	closed	open	Ejection
1	closed	closed	Isovolumic relaxation
3	open	closed	Filling
-	open	open	Not feasible

B. State equations

We will now write the state equations in terms of the x state vector (i.e derive the $A_1(t)$ matrix) for each of these three phases. The $A_2(t)$ matrix can be derived using equation (6).

1) *Isovolumic phase:* In this phase, the aortic and mitral valve are closed, which means D_1 and D_2 are both open-circuit. Moreover, $x_4(t) = 0$. In this case, we have

$$A_1(t) = \begin{bmatrix} \frac{\dot{E}(t)}{E(t)} & 0 & 0 & 0 \\ 0 & -\frac{1}{R_1 C_2} & \frac{1}{R_1 C_2} & 0 \\ 0 & \frac{1}{R_1 C_3} & -\frac{1}{R_1 C_3} & 0 \\ 0 & 0 & 0 & 0 \end{bmatrix} \quad (7)$$

2) *Ejection phase:* As indicated in Table III, D_1 is open-circuit and D_2 is short-circuit. In this phase the left ventricle is pumping blood into the circulatory system, and the following matrix $A_1(t)$ characterizes the system

$$A_1(t) = \begin{bmatrix} \frac{\dot{E}(t)}{E(t)} & 0 & 0 & -E(t) \\ 0 & -\frac{1}{R_1 C_2} & \frac{1}{R_1 C_2} & 0 \\ 0 & \frac{1}{R_1 C_3} & -\frac{1}{R_1 C_3} & \frac{1}{C_3} \\ \frac{1}{L} & 0 & -\frac{1}{L} & -\frac{(R_3+R_4)}{L} \end{bmatrix} \quad (8)$$

3) *Filling phase:* In this phase of the cardiac cycle, D_1 is short-circuit and D_2 is open-circuit, which again implies $x_4(t) = 0$. Therefore, we have

$$A_1(t) = \begin{bmatrix} \frac{\dot{E}(t)}{E(t)} - \frac{E(t)}{R_2} & \frac{E(t)}{R_2} & 0 & 0 \\ \frac{1}{R_2 C_2} & -\frac{(R_1+R_2)}{C_2 R_1 R_2} & \frac{1}{R_1 C_2} & 0 \\ 0 & \frac{1}{R_1 C_3} & -\frac{1}{R_1 C_3} & 0 \\ 0 & 0 & 0 & 0 \end{bmatrix} \quad (9)$$

Note that it can be easily shown that the term $\dot{E}(t)/E(t)$ will not be present in the $A_2(t)$ matrix corresponding to the z state vector. Because of the shape of the elastance function $E(t)$ as shown in figure 2 this term can be the cause of considerable numerical instability. For this reason, in the remainder of this paper we will use the z state vector representation of the cardiovascular model. The $A_2(t)$ matrices corresponding to the three phases are:

4) *Isovolumic phase:*

$$A_2(t) = \begin{bmatrix} 0 & 0 & 0 & 0 \\ 0 & -\frac{1}{R_1 C_2} & \frac{1}{R_1 C_2} & 0 \\ 0 & \frac{1}{R_1 C_3} & -\frac{1}{R_1 C_3} & 0 \\ 0 & 0 & 0 & 0 \end{bmatrix} \quad (10)$$

5) *Ejection phase:*

$$A_2(t) = \begin{bmatrix} 0 & 0 & 0 & -1 \\ 0 & -\frac{1}{R_1 C_2} & \frac{1}{R_1 C_2} & 0 \\ 0 & \frac{1}{R_1 C_3} & -\frac{1}{R_1 C_3} & \frac{1}{C_3} \\ \frac{E(t)}{L} & 0 & -\frac{1}{L} & -\frac{(R_3+R_4)}{L} \end{bmatrix} \quad (11)$$

6) *Filling phase:*

$$A_2(t) = \begin{bmatrix} -\frac{E(t)}{R_2} & \frac{E(t)}{R_2} & 0 & 0 \\ \frac{E(t)}{R_2 C_2} & -\frac{(R_1+R_2)}{C_2 R_1 R_2} & \frac{1}{R_1 C_2} & 0 \\ 0 & \frac{1}{R_1 C_3} & -\frac{1}{R_1 C_3} & 0 \\ 0 & 0 & 0 & 0 \end{bmatrix} \quad (12)$$

III. CARDIOVASCULAR-PUMP MODEL

A model of a left ventricular assist device¹ (LVAD) [12], was connected to the circulatory model shown in Figure 1, which assumes left ventricular cannulation. The addition of the LVAD circuit to the network adds one state variables, flow through the pump, and four passive parameters related to the cannulae.

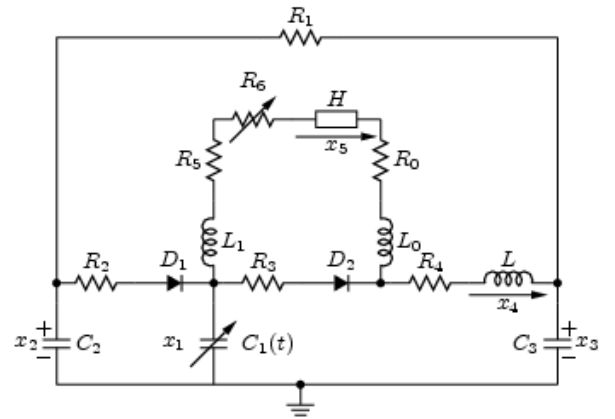


Fig. 3. Cardiovascular-pump Model

The values of inlet and outlet resistance of the cannulae are $R_5 = R_0 = 0.0677$ mmHg.sec/ml, respectively. The inlet and outlet inertance are $L_0 = L_1 = 0.0127$ mmHg.sec²/ml.

¹Nimbus Inc, Rancho Cordova, CA

Resistor R_6 is pressure dependent and simulates the suction phenomena [13].

$$R_6 = \begin{cases} 0 & \text{if } x_1 > P_{th}; \\ -3.5x_1 + 3.5P_{th} & \text{otherwise} \end{cases} \quad (13)$$

where $P_{th} = 1$ mmHg is a threshold. H represents the pressure difference across the pump and is defined by the following characteristic equation, relating pump flow and speed [12]

$$H = \beta_0 Q_P + \beta_1 \frac{dQ_P}{dt} + \beta_2 \omega^2 \quad (14)$$

where $\beta_0 = -0.1707$, $\beta_1 = -0.02177$ and $\beta_2 = 0.0000903$ are the pump model parameters in this case. Notice that the resulting model is a forced system, where the primary control variable is the pump speed.

A. State equations

Now there is an external source of energy in the cardiovascular-pump model. Thus this system is forced, and can be written as

$$\dot{z} = \hat{A}_1(t)z + b_1 u(t) \quad (15)$$

where $u(t) = w^2(t)$ is the control variable and $\hat{A}_1(t)$ can be either a (4×4) or (5×5) time varying matrix, depending on the modes of D_1 and D_2 . The dimension of the scalar vector b_1 , changes accordingly, i.e, it can be (4×1) or (5×1) . The state-vector z is defined as

$$x = [x_1, \dots, x_5]^T = [LVP, LAP, AP, Q_T, Q_P]^T \quad (16)$$

where, Q_T is total flow and Q_P is pump flow. As in the cardiovascular model, it is also possible to define the states of the system as

$$z = [z_1, \dots, z_5]^T = [(LVV - V_0), LAP, AP, Q_T, Q_P]^T \quad (17)$$

and the state vectors x and z are related by the nonlinear transformation $x = Sz$, where the matrix S is

$$S(t) = \begin{bmatrix} E(t) & \vdots & \mathbf{0} \\ \dots & \dots & \dots \\ \mathbf{0} & \vdots & I_n \end{bmatrix} \quad (18)$$

and where I_n is the identity matrix of order $n = 3$ or $n = 4$ depend upon the order of $\hat{A}_1(t)$. Therefore, a similar state equation for z can be derived as $\dot{z} = \hat{A}_2(t)z + b_2 u$, where

$$\hat{A}_2(t) = S^{-1}(t)\hat{A}_1(t)S(t) - S^{-1}(t)\dot{S}(t) \quad (19)$$

$$b_2 = S^{-1}(t)b_1 \quad (20)$$

1) *Isovolumic phase:* As in the heart model, the aortic and mitral valve are closed, which means D_1 and D_2 are open-circuit. However, this time $x_4(t) \neq 0$, but is equal to pump flow, i.e, $x_4(t) = x_5(t)$. In this case, we have

$$A_2(t) = \begin{bmatrix} 0 & 0 & 0 & -1 \\ 0 & -\frac{1}{R_1 C_2} & \frac{1}{R_1 C_2} & 0 \\ 0 & \frac{1}{R_1 C_3} & -\frac{1}{R_1 C_3} & \frac{1}{C_3} \\ \frac{E(t)}{L'+L} & 0 & -\frac{1}{L'+L} & -\frac{R+R_4}{L'+L} \end{bmatrix} \quad (21)$$

for the z vector. Also

$$b_2 = [0 \ 0 \ 0 \ -\beta_2/(L' + L)]^T \quad (22)$$

where

$$L' = L_1 + L_0 + \beta_1 \quad (23)$$

and

$$R = R_5 + R_0 + R_6 + \beta_0 \quad (24)$$

2) *Ejection phase:* As in the previous model, D_2 is short-circuit and D_1 is open-circuit. In this case, we have two flows going into the circulatory system, one from the aorta and the other from the pump. The matrix $\hat{A}_1(t)$ is given by

$$A_2(t) = \begin{bmatrix} 0 & 0 & 0 & -1 & 0 \\ 0 & \frac{-1}{R_1 C_2} & \frac{1}{R_1 C_2} & 0 & 0 \\ 0 & \frac{1}{R_1 C_3} & -\frac{1}{R_1 C_3} & \frac{1}{C_3} & 0 \\ \frac{E(t)}{L} & 0 & -\frac{1}{L} & -\frac{(R_3+R_4)}{L} & \frac{R_3}{L} \\ 0 & 0 & 0 & -\frac{R_3}{L} & \frac{R-R_3}{L} \end{bmatrix} \quad (25)$$

for the z vector and

$$b_2 = [0 \ 0 \ 0 \ 0 \ -\beta_2/L]^T \quad (26)$$

3) *Filling phase:* In this phase of the cardiac cycle, D_1 is short-circuit and $D_2 = 0$ is open-circuit, which again implies $x_5(t) = x_4(t)$. Therefore, we have

$$A_2(t) = \begin{bmatrix} -\frac{E(t)}{R_2} & \frac{1}{R_2} & 0 & -1 \\ \frac{E(t)}{R_2 C_2} & -\frac{(R_1+R_2)}{C_2 R_1 R_2} & \frac{1}{R_1 C_2} & 0 \\ 0 & \frac{1}{R_1 C_3} & -\frac{1}{R_1 C_3} & \frac{1}{C_3} \\ \frac{E(t)}{L'+L} & 0 & -\frac{1}{L'+L} & -\frac{(R+R_4)}{L'+L} \end{bmatrix} \quad (27)$$

for the z vector and

$$b_2 = [0 \ 0 \ 0 \ -\beta_2/(L' + L)]^T \quad (28)$$

IV. SIMULATIONS

In order to assess the capability of the proposed model to emulate left ventricular hemodynamics, tests were performed by simulating the model in MATLAB². Simulations were performed for both nominal steady state conditions, and in response to perturbations of preload and afterload.

Figure 4 shows the simulation waveforms for an adult with heart rate at 75 beats per minute. In that particular case, systolic and diastolic pressure of 115 and 75 mmHg, mean aortic pressure (MAP) of 98 mmHg, cardiac output (CO) was 5.06 l/min and stroke volume (SV) of 67.5 ml/beat. These are consistent with hemodynamic data in normal subjects described in [14].

²The Math Works Inc., Natick, MA

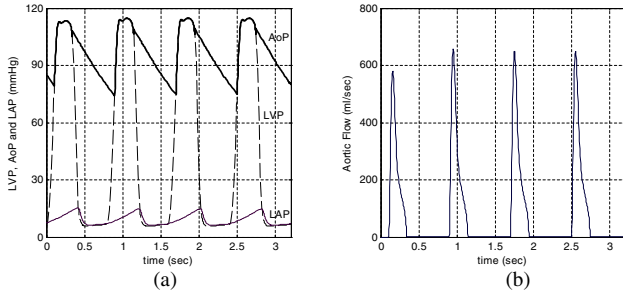


Fig. 4. Simulated hemodynamic waveforms for a normal subject

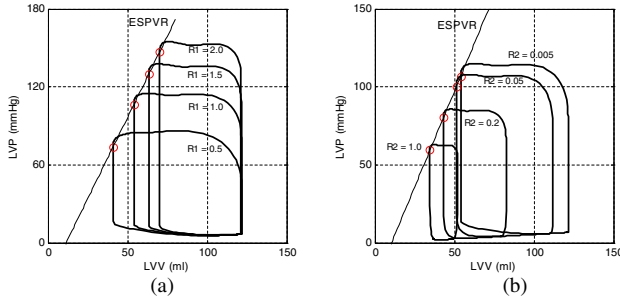


Fig. 5. PV-loops for model validation

A total of 4 preload and 4 afterload conditions were also simulated. In these simulations, we set $E_{max} = 2.5$ mmHg/ml and $V_0 = 10$ ml. The resulting pressure and volume of the ventricle are depicted in the form of pressure-volume (pv)-loops. The pv-loops in Figure 5a, represent the result of changing systemic vascular resistance (R_1), while keeping end diastolic volume (EDV) constant. The pv-loops in Figure 5b depict the result of altering preload conditions by changing the mitral valve resistance (R_2). The slope of the ESPVR (E_{max}) for the loading data in Figure 5a was 2.49 mmHg/ml and V_0 (volume at zero pressure) was 11.02 ml. The linear relationship between pressure and flow is evident for the ESPVR, since the correlation coefficient between those two variables was 0.99. As for preload changes (Figure 5b), the slope of ESPVR was 2.45 mmHg/ml for ESPVR, V_0 was 10.45ml, and a correlation coefficient of 0.99.

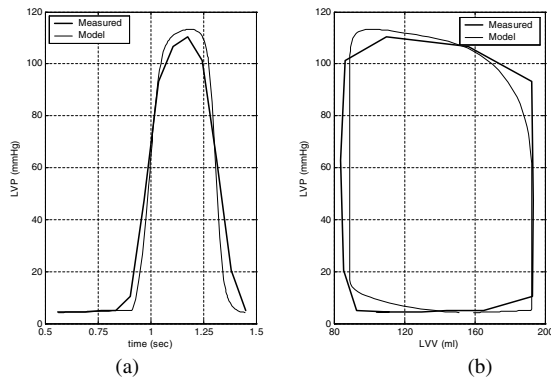


Fig. 6. Curve fitting using human clinical data

Figure 6 shows an example of curve fitting to human clinical data, using the heart model. We estimated the parameters for a patient suffering from cardiomyopathy, from pressure and volume data and used those parameters in our simulations. For LVP fitting test, we found an error of 4.4% calculated as the ratio of the squared error to the square measured value. For the pv-loop test, we compare the stroke work (area of the pv-loop, SW) of the patient with that generated by the model. The first was 10,690 mmHg.ml and the second 10,201 mmHg.ml, which represents a difference of 4.5%.

A. Cardiovascular-pump model response

Once the cardiovascular model was validated, tests were performed to assess the open-loop response of the cardiovascular-pump model shown in Figure 3. As the pump speed is increased (see Figure 7(a)), the amplitude of oscillation gradually decreases, while net flow increases. Beyond the point of maximum flow, the waveform exhibits sudden negative spikes, indicative of suction. (See Figure 7(c)).

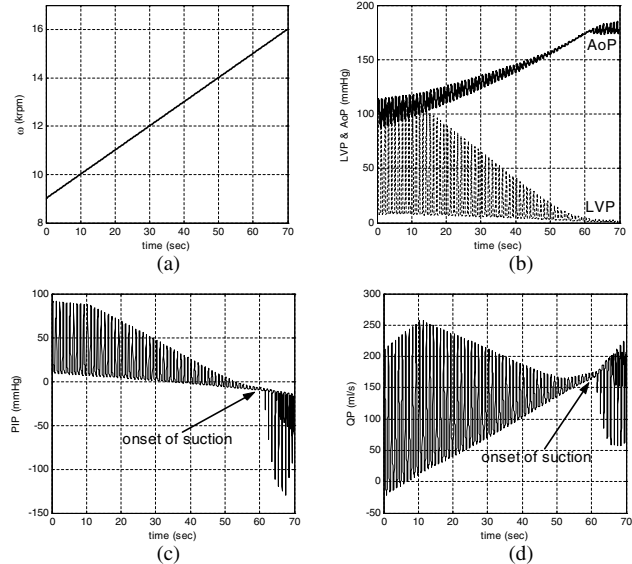


Fig. 7. (a) Speed profile, (b) AoP and LVP pressures, (c) Pump Inlet Pressure and (d) Pump Flow

During ejection, theoretically, there are two paths for the flow out the ventricle, either through the aortic valve or through the pump. However, the aortic valve does not open if the left ventricular pressure is lower than the aortic pressure. This is usually the case, since the pump decreases the internal pressure in the ventricle. Whether the aortic valve will open or not, depends on the pump speed and on how “strong” (contractility state) the heart really is [12]. This situation is evident in Figure 7(b), where the aortic valve remains closed, for $t \geq 10$ sec. The mitral valve likewise will remain open if the pump drains sufficient flow to cause ventricular pressure to fall below atrial pressure.

Another test investigated how hemodynamic variables were affected as systemic vascular resistance changes. To simulate a “weak” heart, the value of E_{max} was set to 0.7,

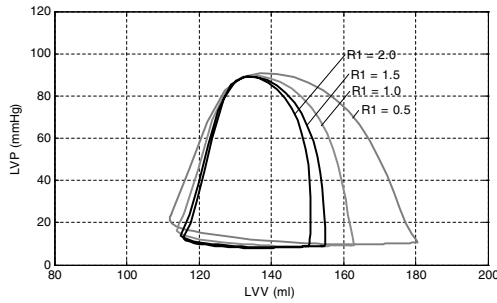


Fig. 8. PV-loops for model validation

TABLE IV
HEMODYNAMIC PARAMETERS FOR $E_{max} = 0.7$

R_1	SV (ml)	CO (l/min)	AoP (mmHg) Sys / Dia / Mean	LAP (mmHg) Max / Mean / Min
0.5	68.67	5.1	101 / 69 / 88	22 / 15 / 9
1.0	49.01	3.6	114 / 85 / 100	17 / 11 / 9
1.5	39.89	2.99	120 / 87 / 107	15 / 10 / 8
2.0	35.20	2.64	124 / 88 / 110	13 / 10 / 8

approximately 1/3 of its nominal value ($E_{max} = 2.0$). In all simulations, we ran the cardiovascular-pump model by incrementing the speed as a ramp from 9,000 rpm to 10,000 rpm in 20 seconds. Table IV shows the hemodynamic values found at steady state in those tests and Figure 8 shows the PV loops.

V. CONCLUSION

We presented a nonlinear coupled cardiovascular-pump model and its characterization in state space form. That particular representation is suitable for the design of pump speed controllers using modern control techniques. The suction phenomena, due to overpumping, can also be studied by using this model. A simple capacitance represents the pulmonary circulation and left atrium in our proposed model. It is difficult to obtain reliable measurements for the high pressure system (left ventricle), and is even harder to measure those variables (pressures and flows) in the right side of the human heart. Since this model is univentricular, it may be suitable for studying physiological phenomena associated with hypoplastic heart syndrome (univentricular heart).

A more accurate model for the elastance function, which takes into account the nonlinear behavior of EDPVR is currently being developed as well as a baroreflex system to accommodate variations in heart rate and systemic vascular resistance due to MAP changes. Moreover, a gradient based feedback controller has been developed to automatically adjust the pump speed to meet the patient's blood flow requirements up to the point where suction may occur [15]. At that point the controller will maintain a constant pump speed keeping the gradient of the minimum pump flow at zero. Simulation results have shown the feasibility of this approach.

VI. ACKNOWLEDGMENTS

Antonio Ferreira gratefully acknowledges the Alcoa Foundation Maranhao, Brazil Engineering Fellowship Program and the Foundation of Research of the State of Maranhao/Brazil - FAPEMA. The authors wish to thank Dr. S. Vandenberghe for kindly providing the clinical data used in this research project.

REFERENCES

- [1] M. Zacek and E. Krause, "Numerical simulation of the blood flow in the human cardiovascular system," *J. Biomechanics*, vol. 29, no. 1, pp. 13–20, 1996.
- [2] S. Voytik, C. Babbs, and S. Badylak, "Simple electrical model of the circulation to explore design parameters for a skeletal muscle ventricle," *Journal of Heart Transp.*, vol. 9, no. 2, pp. 160–174, 1990.
- [3] G. Avanzolini *et al.*, "Cades simulation of the closed-loop cardiovascular system," *Int. J. Biomed. Comput.*, vol. 18, pp. 39–49, 1988.
- [4] J. Bai, K. Ying, and D. Jaron, "Cardiovascular responses to external counterpulsation: a computer simulation," *Journal of Heart Transp.*, vol. 30, pp. 317–323, 1992.
- [5] C. D. Lazzari, G. Ferrari, R. Mimmo, G. Tosti, and D. Ambrosi, "A desktop computer model of the circulatory system for assistance simulation: effect of an lvad on energetic relationships inside the left ventricle," *Med. Eng. Phys.*, vol. 16, pp. 97–103, 1994.
- [6] L. Xu and M. Fu, "Computer modeling of interactions of an electric motor, circulatory system and rotary blood pump," *ASAIO J.*, vol. 46, no. 5, pp. 604–611, 2000.
- [7] M. Vollkron, H. Schima, L. Hubber, and G. Wieselthler, "Interactions of the cardiovascular system with an implanted rotary assist device: Simulation study with a refined computer model," *Intern. Soc. for Art. Organs*, vol. 26, no. 4, pp. 349–359, 2002.
- [8] D. S. Breitenstein, "Cardiovascular modeling: the mathematical expression of blood circulation," Master's thesis, University of Pittsburgh, PA, 1993.
- [9] Y.C. Yu, J. Boston, M. Simaan, and J. Antaki, "Estimation of systemic vascular bed parameters for artificial heart control," *IEEE Trans. Automat. Contr.*, vol. 43, pp. 765–777, June 1998.
- [10] H. Suga and K. Sagawa, "Instantaneous pressure-volume relationships and their ratio in the excised, supported canine left ventricle," *Circ Res*, vol. 35, no. 1, pp. 117–126, 1974.
- [11] N. Stergiopoulos, J. Meister, and N. Westerhof, "Determinants of stroke volume and systolic and diastolic aortic pressure," *Am J Physiol.*, vol. 270, no. 6 Pt 2, pp. H2050–2059, 1996.
- [12] S. Choi, "Modeling and control of left ventricular assist system," Ph.D. dissertation, University of Pittsburgh, Pittsburgh, PA, May 1998.
- [13] H. Shima, J. Honigschnable, W. Trubel, and H. Thoma, "Computer simulation of the circulatory system during support with a rotary blood pump," *Tran Am Soc Artif Intern Org*, vol. 36, pp. M252–M254, 1990.
- [14] A. Guyton and J. E. Hall, *Textbook of Medical Physiology*. Philadelphia, PA: W. B. Saunders Co., 1996.
- [15] A. Ferreira, S. Chen, D. Galati, M.A. Simaan, and J.F. Antaki, "A dynamic state space representation and performance analysis of a feedback controlled rotary left ventricular assist device," *To appear in the Proc. of the ASME 2005 - International Mechanical Engineering Congress and Exposition*, Orlando, USA, November 5–11, 2005.